Proceedings of the ASME 2013 International Design Engineering Technical Conferences &
Computers and Information in Engineering Conference
IDETC/CIE 2013
August 4-August 7, 2013, Portland, OR, USA

DETC2013-12594

DYNAMICS OF DRILL BITS WITH CUTTING EDGES OF VARYING PARAMETERS

Zoltan Dombovari*
Department of Applied Mechanics
Budapest University of Technology and Economics
Budapest, H-1521
Hungary
Email: dombo@mm.bme.hu

Gabor Stepan
Department of Applied Mechanics
Budapest University of Technology and Economics
Budapest, H-1521
Hungary
Email: stepan@mm.bme.hu

ABSTRACT

In the metal cutting industry it is well known that milling processes can be stabilized by applying different strategies in order to destroy the pure single delay regeneration that arise in case of conventional milling tools when high material removal rates are used either at low or at high cutting speeds. To achieve this goal, variable pitch angle, variable helix angle and serrated tools are already available in the market and serve alternative solutions for process designers to enhance milling process stability. Regeneration can occur and can cause instability on the tip of the deep drilling equipment when the drill bit is driven across hard earth crust materials. This work shows that theories introduced for milling processes can be implemented to improve the stability properties of deep drilling processes, too. Unlike in case of most milling processes, however, the stability properties of deep drilling are affected by the longitudinal and the torsional vibration modes. In this paper, the geometrical and mechanical models are derived for drill bits with general shapes of cutting edges and it is shown that the two DOF dynamics can be described by distributed state dependent delay differential equations. The stability properties are characterized in stability diagrams that can help to select the optimal drilling process parameters.

INTRODUCTION

It has became clear that future industry cannot be based on easily accessible fossil energy resources for long time. One possible solution is to replace our energy needs with renewable resources. Unfortunately, this transition cannot be carried out instantly due to engineering, economical and scientific problems still to be solved. In case of an ideal solution, during the transition period, the fossil fuels still remain a major but gradually decreasing portion of our energy consumption. Considering oil and gas reserves the 'easy time' is over, new solutions need to be considered to extract fuel from shale gas, oil sand and difficult-to-reach oil reserves.

To exploit these possibilities, the conventional way of drilling needs to be improved in oil drill technology in order to access difficult-to-reach resources. The dynamic investigation of the entire drill rig contributes to the optimization and improvement of the drilling process. Many different dynamic problems arise in deep drilling including forced vibrations [1] and self-excited vibrations [2]. The most difficult problems involve the self-excited vibrations like stick-slip [3, 4]. In this work we focus on the dynamic instabilities that are caused by the cutting process itself through the so-called regenerative effect.

Drilling, turning, milling are processes that are subjected to regenerative effect [5, 6] due to the cut surface pattern that continuously stores the relative vibration between the tool and the workpiece. Because of the rotating tool (or workpiece), the past state of the tool excites the system after a certain time. This effect can cause instability of the expected stationary drilling operation.

The regeneration can be described by a functional differential equation (FDE) [7], more specifically by its retarded type [8]. In the case of turning and drilling, the governing equation is

*Address all correspondence to this author.

autonomous, but milling has time-periodic coefficients [9], too. This equation generates an infinite dimensional phase space similarly to the partial differential equations [7], which require special (analytical and numerical) techniques to investigate [10]. Moreover, in the case of variable helix geometry, the system can be described by distributed delays, that is, delays act on the system with continuously varying strength, described by the so-called weight distribution function [11].

In this study, we show that deep drill bits with variable helix can be described by distributed DDEs [11]. In this way we obtain an insight to the intricate dynamics of variable helix drill bits and those parameter domains are identified where the drilling process has improved stability properties. In the same time, parameter domains are also found where the unstable drilling appears spontaneously providing percussive drilling [12].

In the first section, we construct the geometric model of drill bits with constant helix variation. In the subsequent mechanical model, linear cutting force characteristics is considered acting along the cutting edges. Finally, stability calculations are performed using the analytical formulation of the characteristic equation of the system.

MECHANICS OF VARIABLE HELIX DRILL BIT

In this section an ideal spherical geometry is considered with variable helical edges on. The description of the angular positions between subsequent edges are the key point to determine the regeneration(s) that affect(s) the drill bit dynamics.

Spherical Helix Geometry

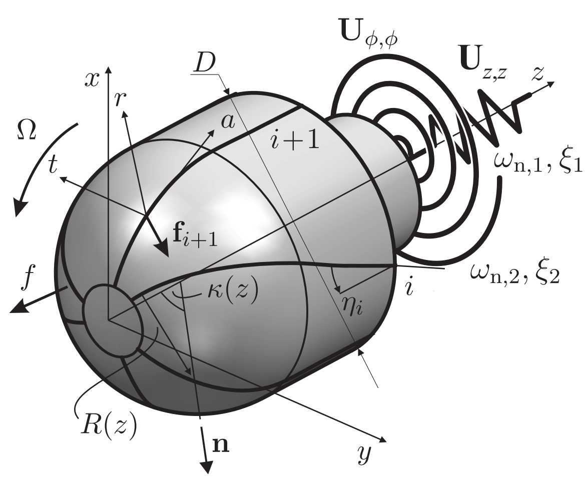

FIGURE 1. THE SKETCH OF THE DRILL BIT WITH VARIED CONSTANT HELIX ANGLES.

Fig. 1 shows the geometry considered in this work, that models a spherical envelope of the drill bit. The edges start at axial level z_0 with initial pitch angles $\varphi_{p,i,0}$ between subsequent edges. The constant, but non-uniform helix angles shift the angular positions by the so-called lag-angle $\varphi_{\eta,i}(z)$ compared to the initial angular positions $\sum_{i=1}^{k-1} \varphi_{p,i,0}$ $(k = 1, 2, \ldots Z)$, where Z is the number of edges. This lag angle has a differential relationship with the helix angle as

$$\varphi'_{\eta,i}(z) = \frac{\tan \eta_i}{R(z) \sin \kappa(z)}, \tag{1}$$

where $R(z)$ and $\kappa(z)$ are the envelope diameter and the lead angle w.r.t. the axial coordinate z. Straightforwardly, these have also differential relationship as

$$R'(z) = \cot \kappa(z), \tag{2}$$

when

$$R(z) = \sqrt{\left(\tfrac{D}{2}\right)^2 - \left(z - \tfrac{D}{2}\right)^2} \tag{3}$$

and D is the diameter of the ideal hemisphere. Afterwards, the pitch angles between subsequent edges w.r.t. the axial coordinate z are

$$\varphi_{p,i}(z) = \varphi_{p,i,0} + \varphi_{\eta,i}(z) - \varphi_{\eta,i+1}(z). \tag{4}$$

Substituting (1) into (4) the pitch angles have the form

$$\varphi_{p,i}(z) = \varphi_{p,i,0} + (\tan \eta_i - \tan \eta_{i+1}) \int_{z_0}^{D/2} \frac{\mathrm{d}z}{R(z) \sin \kappa(z)}. \tag{5}$$

With further substitution of (2) and (3) into (5) the pitch angles on the hemisphere can be expressed in a close form after some algebraic manipulations

$$\varphi_{p,i}(z) = \varphi_{p,i,0} + (\tan \eta_i - \tan \eta_{i+1}) \frac{1}{2} \ln \frac{z}{z_0} \frac{D - z_0}{D - z}, \tag{6}$$

using

$$\sin \kappa(z) = \frac{1}{\sqrt{R'^2(z) + 1}}. \tag{7}$$

Regenerative Force on the Drill Bit

The drill bit in this investigation has axial and torsional modes described by $\zeta(t)$ and $\phi(t)$ general coordinates as relative motions to the drill bit axial and angular position (see Fig. 1)

$$\varphi_i(z,t) = \Omega t + \phi(t) + \sum_{k=1}^{i-1} \varphi_{\mathrm{p},k}(z) - \varphi_{\eta,1}(z). \tag{8}$$

The chip thickness that excites the system is derived as a projection of the edge segment's movement $\mathbf{r}_i(z,t)$ related to the same angular positions $\varphi_i(z,t)$ of subsequent edge segments as

$$h_i(z,t) \approx \mathbf{r}_i(z,t)\mathbf{n}_i(z). \tag{9}$$

The local movement of subsequent edge portions and the local normal vectors of the edges can be expressed as

$$\mathbf{r}_i(z,t,\zeta_t) := \mathbf{r}_i(z,t) = \begin{bmatrix} 0 \\ 0 \\ \Delta\zeta_i(t) - f\frac{\Omega}{2\pi}\tau_i \end{bmatrix}, \tag{10}$$

$$\mathbf{n}_i(z) = \begin{bmatrix} \sin\kappa(z)\sin\varphi_i(z,t) \\ \sin\kappa(z)\cos\varphi_i(z,t) \\ -\cos\kappa(z) \end{bmatrix}. \tag{11}$$

The regeneration in (10) is $\Delta\zeta_i(t) = \zeta(t) - \zeta(t-\tau_i)$ where τ_i is the (delay-) time needed for the next edge to be at the angular position of the previous edge. Accordingly, (10) does not only depend on the present motion it does on the past motion too, described by the shift $\zeta_t := \zeta_t(\theta) = \zeta(t+\theta)$ ($\theta \in [-\chi, 0)$ and χ is the largest possible delay). The time delay can be expressed in the following implicit form considering the perturbation on the constant angular velocity Ω of the drill bit by the torsional mode $\phi(t)$

$$\varphi_{\mathrm{p},i}(z) = \int_{t-\tau_i}^{t} \Omega + \dot{\phi}(t)\mathrm{d}t = \Omega\tau_i + \phi(t) - \phi(t-\tau_i). \tag{12}$$

From this equation one can recognize the delay must be z dependent. It is also time dependent but through the torsional present and past motions, thus, this delay is actually state dependent. The following is used henceforth to ease the notation $\tau_i(z,\phi_t) = \tau_i$, ($\phi_t := \phi_t(\theta) = \phi(t+\theta)$), thus $\mathbf{r}_i(z,t,\zeta_t,\tau_i(z,\phi_t)) = \mathbf{r}_i(z,t,\zeta_t)$ and $\Delta\zeta_i(t,\tau_i(z,\phi_t)) = \Delta\zeta_i(t)$. Then the regenerative chip thickness can be expressed after (9) as

$$\begin{aligned} &h_i(z,t,\zeta_t,\tau_i(z,\phi_t)) \\ &\quad = -\cos\kappa(z)\Delta\zeta_i(t,\tau_i(z,\phi_t)) + \cos\kappa(z) f\frac{\Omega}{2\pi}\tau_i(z,\phi_t). \end{aligned}$$

The local specific force can be determined in the local t (tangential), r (radial) and a (axial) coordinate system (tra), that is,

$$\mathbf{f}_{tra,i}(z,t,\zeta_t,\tau_i(z,\phi_t)) = -(\mathbf{K}_\mathrm{e} + \mathbf{K}_\mathrm{c} h_i(z,t,\zeta_t,\tau_i(z,\phi_t))),$$

where $\mathbf{K}_\mathrm{e}$ and $\mathbf{K}_\mathrm{c}$ are the edge and cutting coefficients of the material being cut. The specific force can be rewritten in Cartesian system using the following transformation

$$\mathbf{f}_i(z,t,\zeta_t,\tau_i(z,\phi_t)) = \mathbf{T}_i(z,t)\mathbf{f}_{tra,i}(z,t,\zeta_t,\tau_i(z,\phi_t)),$$

where $\mathbf{T}_i(z,t)$ is the transformation matrix [13] between the (tra) and the (xyz) system. This results the following specific forces in the axial z and tangential t direction

$$\begin{aligned} f_{z,i}(z,t,\zeta_t,\tau_i(z,\phi_t)) = &\cos\kappa(z)(K_{\mathrm{e},r} + K_{\mathrm{c},r}h_i) \\ &- \sin\kappa(z)(K_{\mathrm{e},a} + K_{\mathrm{c},a}h_i), \end{aligned} \tag{13}$$

$$f_{t,i}(z,t,\zeta_t,\tau_i(z,\phi_t)) = -K_{\mathrm{e},t} - K_{\mathrm{c},t}h_i, \tag{14}$$

that excite the axial and rotational modes, respectively and $h_i := h_i(z,t,\zeta_t,\tau_i(z,\phi_t))$. The sum of all specific force components along the edges and for all flutes gives the resultant cutting force and torque

$$\begin{aligned} F_z(t,\zeta_t,\phi_t) &= \sum_{i=1}^{Z}\int_{z_0}^{D/2} \frac{f_{z,i}(z,t,\zeta_t,\tau_i(z,\phi_t))}{\cos\eta_i \sin\kappa(z)}\mathrm{d}z, \\ M_\phi(t,\zeta_t,\phi_t) &= -\sum_{i=1}^{Z}\int_{z_0}^{D/2} \frac{R(z) f_{t,i}(z,t,\zeta_t,\tau_i(z,\phi_t))}{\cos\eta_i \sin\kappa(z)}\mathrm{d}z. \end{aligned} \tag{15}$$

Drill Bit Dynamics

Considering the longitudinal ζ and the rotational modes ϕ and modal force ($U_{z,z}F_z(t,\zeta_t,\phi_t)$) and modal torque ($U_{\phi,\phi}M_\phi(t,\zeta_t,\phi_t)$) excitations, the deep drilling process is derived in modal space. Unlike the milling process [14] the governing equations of the system are autonomous and have the following form

$$\begin{aligned} &\ddot{q}_k(t) + 2\xi_k\omega_{\mathrm{n},k}\dot{q}_k(t) + \omega_{\mathrm{n},k}^2 q_k(t) \\ &\quad = \sum_{i=1}^{Z}\int_{z_0}^{D/2} g_{k,i}(q_1(t), q_1(t-\tau_i(z,q_{2,t})), \tau_i(z,q_{2,t}))\mathrm{d}z, \quad k=1,2, \end{aligned} \tag{16}$$

with

$$g_{1,i}(q_1(t), q_1(t-\tau_i(z,q_{2,t})), \tau_i(z,q_{2,t})) = U_{z,z}\frac{f_{z,i}(z,t,\zeta_t,\tau_i(z,\phi_t))}{\cos\eta_i \sin\kappa(z)}, \tag{17}$$

$$g_{2,i}(q_1(t), q_1(t-\tau_i(z,q_{2,t})), \tau_i(z,q_{2,t})) = -U_{\phi,\phi}\frac{R(z) f_{t,i}(z,t,\zeta_t,\tau_i(z,\phi_t))}{\cos\eta_i \sin\kappa(z)}, \tag{18}$$

and with the implicit algebraic condition for the delay in the interval of the axial coordinate $z \in [z_0, D/2]$.

$$\varphi_{\mathrm{p},i}(z) = \Omega\tau_i(z,q_{2,t}) + U_{\phi,\phi}(q_2(t) - q_2(t-\tau_i(z,q_{2,t}))). \tag{19}$$

In (16-19) $\zeta(t) = U_{z,z}q_1(t)$ and $\phi(t) = U_{\phi,\phi}q_2(t)$, where $q_k(t)$'s ($\sqrt{\mathrm{kg}}\,\mathrm{m}$) ($k = 1,2$) are the modal coordinates. At the equilibrium, $q_1(t) = \overline{q}_1 + x_1(t)$ and $q_2(t) = \overline{q}_2 + x_2(t)$. Thus

$$\begin{aligned}\overline{q}_1 &= \frac{U_{z,z}}{\omega_{\mathrm{n},1}^2}\sum_{i=1}^{Z}\int_{z_0}^{D/2}\frac{f_{z,i,0}(z)}{\cos\eta_i\sin\kappa(z)}\mathrm{d}z,\\ \overline{q}_2 &= \frac{U_{\phi,\phi}}{\omega_{\mathrm{n},2}^2}\sum_{i=1}^{Z}\int_{z_0}^{D/2}\frac{R(z)f_{t,i,0}(z)}{\cos\eta_i\sin\kappa(z)}\mathrm{d}z,\end{aligned} \tag{20}$$

where

$$\begin{aligned}f_{z,i,0}(z) &= -\sin\kappa(z)K_{\mathrm{e},a} + \cos\kappa(z)K_{\mathrm{e},r}\\ &\quad + (\cos\kappa(z)K_{\mathrm{c},r} - \sin\kappa(z)K_{\mathrm{c},a})\cos\kappa(z) f\frac{\Omega}{2\pi}\overline{\tau}_i(z),\\ f_{t,i,0}(z) &= K_{\mathrm{e},t} + K_{\mathrm{c},t}\cos\kappa(z) f\frac{\Omega}{2\pi}\overline{\tau}_i(z),\end{aligned} \tag{21}$$

and $\overline{\tau}_i(z) = \varphi_{\mathrm{p},i}(z)/\Omega$ after (19). Then the associated linear system around the stationary solutions $\overline{q}_1$ and $\overline{q}_2$ is

$$\begin{aligned}&\ddot{x}_k(t) + 2\xi_k\omega_{\mathrm{n},k}\dot{x}_k(t) + \omega_{\mathrm{n},k}^2 x_k(t)\\ &\quad = \sum_{i=1}^{Z}\int_{z_0}^{D/2}\mathrm{D}_1 g_{k,i}(\overline{q}_1,\overline{q}_1,\overline{\tau}_i(z))x_1(t)\\ &\qquad + \mathrm{D}_2 g_{k,i}(\overline{q}_1,\overline{q}_1,\overline{\tau}_i(z))x_1(t-\overline{\tau}_i(z))\\ &\qquad + (\mathrm{D}_3 g_{k,i}(\overline{q}_1,\overline{q}_1,\overline{\tau}_i(z))\mathrm{D}_{\mathbf{q}_t(\theta)}\tau_i)\mathbf{x}_t(\theta)\mathrm{d}z,\\ &\quad k = 1,2.\end{aligned} \tag{22}$$

In (22) $\mathrm{D}_l g_{k,i}$ means partial derivative w.r.t. the lth argument of $g_{k,i}$ and $\mathrm{D}_{\mathbf{q}_t(\theta)}\tau_i$ symbolizes the Frechet derivative of the state-dependent delays by the state $\mathbf{q}_t(\theta)$ itself. Considering the arguments of the integrals in the right-hand-side at (17,18) and the implicit condition at (19) the different derivative terms are listed below

$$\mathrm{D}_1 g_{1,i} = -\mathrm{D}_2 g_{1,i} = -U_{z,z}\frac{\cos\kappa(z)K_{\mathrm{c},r} - \sin\kappa(z)K_{\mathrm{c},a}}{\cos\eta_i\tan\kappa(z)}, \tag{23}$$

$$\mathrm{D}_1 g_{2,i} = -\mathrm{D}_2 g_{2,i} = -U_{\phi,\phi}\frac{R(z)K_{\mathrm{c},t}}{\cos\eta_i\tan\kappa(z)}, \tag{24}$$

$$\mathrm{D}_3 g_{1,i} = U_{z,z}\frac{\cos\kappa(z)K_{\mathrm{c},r} - \sin\kappa(z)K_{\mathrm{c},a}}{\cos\eta_i\tan\kappa(z)} f\frac{\Omega}{2\pi}, \tag{25}$$

$$\mathrm{D}_3 g_{2,i} = U_{\phi,\phi}\frac{R(z)K_{\mathrm{c},t}}{\cos\eta_i\tan\kappa(z)} f\frac{\Omega}{2\pi}, \tag{26}$$

$$\mathrm{D}_{\mathbf{q}_t(\theta)}\tau_i = \begin{cases} -\frac{U_{\phi,\phi}}{\Omega}, & \text{if } \theta = 0,\\ \frac{U_{\phi,\phi}}{\Omega}, & \text{if } \theta = -\tau_i(z,q_{2,t}),\\ 0, & \text{otherwise.}\end{cases} \tag{27}$$

These lead to the following dimensionless form of the system

$$\begin{aligned}&x_1''(t) + 2\xi_1 x_1'(t) + (1+\delta c_1)x_1(t) + \frac{\varepsilon_3}{2\pi}\psi\delta c_1 x_2(t)\\ &\quad = \delta\sum_{i=1}^{Z}\int_{z_0}^{1/2} c_{1,i}(z)x_1(t-\overline{\tau}_i(z)) + \frac{\varepsilon_3}{2\pi}\psi c_{1,i}(z)x_2(t-\overline{\tau}_i(z))\mathrm{d}z,\end{aligned} \tag{28}$$

$$\begin{aligned}&x_2''(t) + 2\varepsilon_1\varepsilon_2\xi_1 x_2'(t) + \left(\varepsilon_1^2 + \frac{\varepsilon_3^2}{2\pi}\delta\psi c_2\right)x_2(t) + \varepsilon_3\delta c_2 x_1(t)\\ &\quad = \varepsilon_3\delta\sum_{i=1}^{Z}\int_{z_0}^{1/2} c_{2,i}(z)x_1(t-\overline{\tau}_i(z)) + \frac{\varepsilon_3}{2\pi}\psi c_{2,i}(z)x_2(t-\overline{\tau}_i(z))\mathrm{d}z,\end{aligned} \tag{29}$$

using the following transformations and parameters

$$\omega_{\mathrm{n},1}t \to t, \quad U_{z,z}\frac{x_k(t)}{D} \to x_k(t), \quad \frac{z}{D} \to z, \tag{30}$$

$$\varepsilon_1 := \frac{\omega_{\mathrm{n},2}}{\omega_{\mathrm{n},1}}, \quad \varepsilon_2 := \frac{\xi_2}{\xi_1}, \quad \varepsilon_3 := D\frac{U_{\phi,\phi}}{U_{z,z}}, \tag{31}$$

$$\delta := U_{z,z}^2\frac{DK_{\mathrm{c},r}}{\omega_{\mathrm{n},1}^2}, \quad \vartheta_1 := \frac{K_{\mathrm{c},a}}{K_{\mathrm{c},r}}, \quad \vartheta_2 := \frac{K_{\mathrm{c},t}}{K_{\mathrm{c},r}}, \tag{32}$$

$$c_{1,i}(z) = \frac{\cos\kappa(z) - \vartheta_1\sin\kappa(z)}{\cos\eta_i\tan\kappa(z)}, c_{2,i}(z) = \frac{\rho(z)\vartheta_2}{\cos\eta_i\tan\kappa(z)}, \tag{33}$$

$$\rho(z) := \frac{R(z)}{D}, \quad \psi := \frac{f}{D}. \tag{34}$$

Also considering (30), the followings hold: $\omega_{\mathrm{n},1}\overline{\tau}_i(z) \to \overline{\tau}_i(z)$ and $z_0/D \to z_0$. This can be reformulated using matrix form as

$$\mathbf{x}''(t) + \mathbf{D}\mathbf{x}'(t) + (\mathbf{K} + \delta\mathbf{C})\mathbf{x}(t) = \delta\sum_{i=1}^{Z}\int_{z_0}^{1/2}\mathbf{C}_i(z)\mathbf{x}(t-\overline{\tau}_i(z))\mathrm{d}t, \tag{35}$$

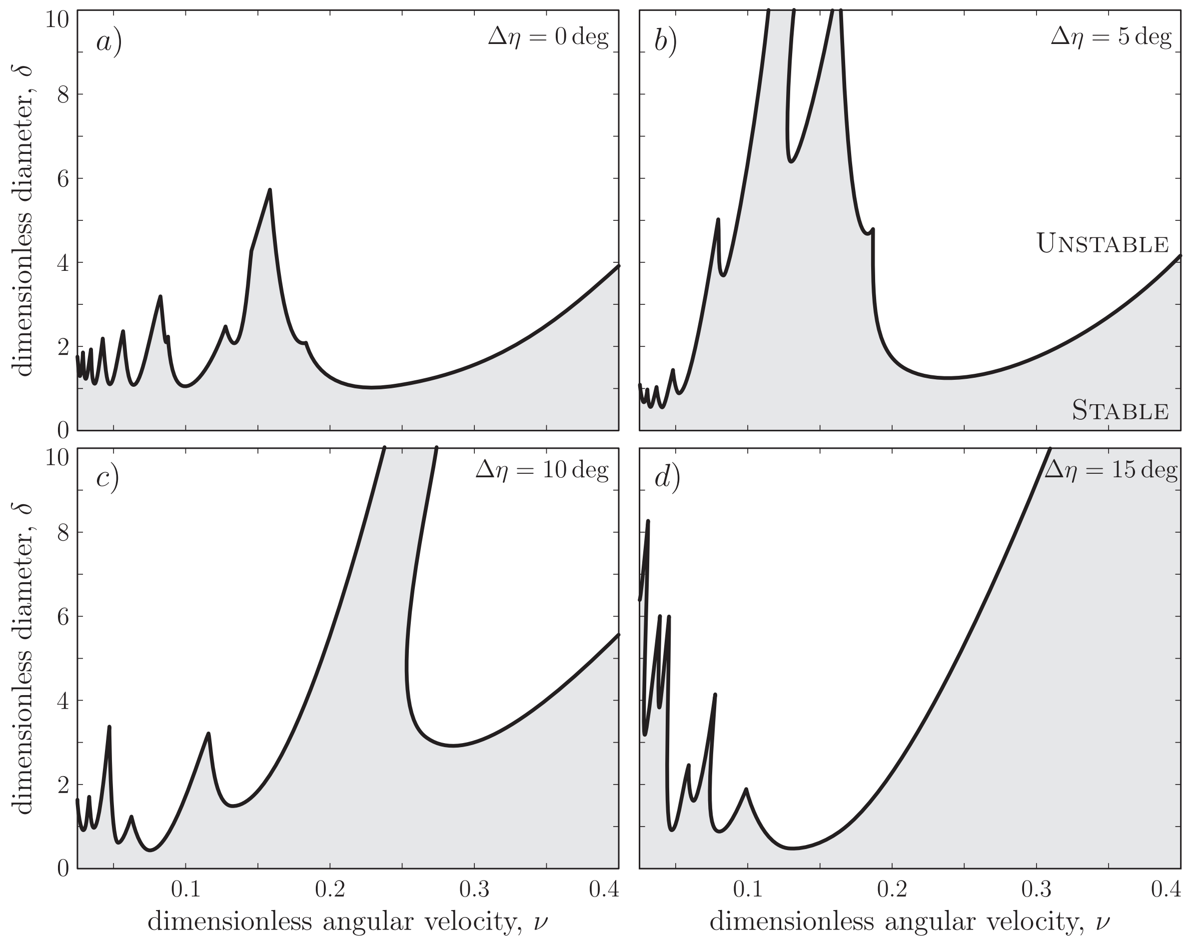

FIGURE 2. THE EFFECT OF HELIX VARIATION ON STABILITY

where

$$\mathbf{D} = \mathrm{diag}(2\xi_1, 2\varepsilon_1\varepsilon_2\xi_1), \quad \mathbf{K} = \mathrm{diag}(1, \varepsilon_1^2),$$
$$\mathbf{C}_i(z) = \begin{bmatrix} c_{1,i}(z) & \frac{\varepsilon_3}{2\pi}\psi c_{1,i}(z) \\ \varepsilon_3 c_{2,i}(z) & \frac{\varepsilon_3^2}{2\pi}\psi c_{2,i}(z) \end{bmatrix}, \quad \mathbf{C} = \sum_{i=1}^{Z}\int_{z_0}^{1/2}\mathbf{C}_i(z)\mathrm{d}z. \tag{36}$$

Substituting $\mathbf{x}(t) = \mathbf{b}\mathrm{e}^{\lambda t}$ general solution, the following term of the characteristic equation of the system is formulated that determines the asymptotic stability of $\overline{q}_1$ and $\overline{q}_2$ stationary solutions:

$$\det\left(\mathbf{I}\lambda^2 + \mathbf{D}\lambda + (\mathbf{K}+\delta\mathbf{C}) - \delta\sum_{i=1}^{Z}\int_{z_0}^{1/2}\mathbf{C}_i(z)\mathrm{e}^{-\lambda\overline{\tau}_i(z)}\mathrm{d}z\right) = 0. \tag{37}$$

Stability boundaries that relate to Hopf bifurcation can be found with $\lambda = \mathrm{i}\omega$ substitution. This results in a transcendental algebraic equation for the vibration frequency ω.

STABILITY BEHAVIOUR

The stability behaviour of a drill bit is investigated in this section. The considered drill bit has six edges ($Z = 6$), the initial level where the edges start is $z_0 = 0.1$. The base helix angle is $\eta = 20\,\mathrm{deg}$ and the varying constant helices are set as

$$\eta_i = (\eta, \eta+\Delta\eta, \eta, \eta+\Delta\eta, \eta, \eta+\Delta\eta), \quad \Delta\eta = \eta_{i+1} - \eta_i. \tag{38}$$

The initial pitch angles are selected to have uniform pitches at the $z = 1/2$ level using (6), that is

$$\varphi_{\mathrm{p},i,0} = \frac{2\pi}{Z} + (\tan\eta_{i+1} - \tan\eta_i)\frac{1}{2}\ln\frac{1-z_0}{z_0}. \tag{39}$$

In order to carry out the stability investigations the following parameters are needed: $\xi_1 = 0.05$, $\varepsilon_1 = 3$, $\varepsilon_2 = 0.5$, $\varepsilon_3 = 3$, $\vartheta_1 = 0.6$, $\vartheta_2 = 0.3$ and $\psi = 0.001$.

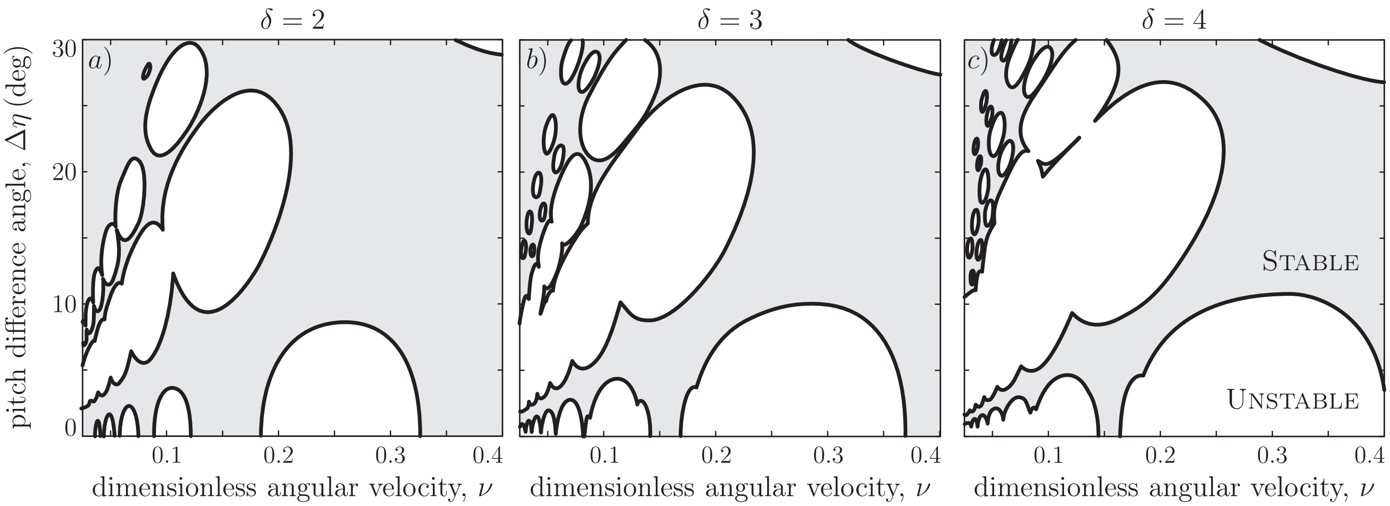

FIGURE 3. THE EFFECT OF PITCH DIFFERENCE ON STABILITY

Stability charts are presented in Fig. 2 in the space of dimensionless angular velocity $\nu = \Omega/\omega_{n,1}$ and the dimensionless drill bit diameter δ (32). The stability charts were calculated using high dimensional bisection method [15] on the characteristic equation, when $\lambda = \mathrm{i}\omega$. It can be followed the stability can change w.r.t. the dimensionless diameter and the angular velocity. Sweet spots may arise with the change of the pitch difference angle $\Delta\eta$, which effect gives possibility for tool geometry optimization.

This effect further investigated in Fig. 3 and stability charts are created in the space of the dimensionless angular velocity ν and the pitch difference angle $\Delta\eta$. Special lens-like stability behaviour can be traced in these intersections of the stability charts presented in Fig. 2 for the following dimensionless diameters $\delta = 2, 4, 6$. These instability lenses seem to be situated along a tilted lines and through these lenses sometimes connected too.

Analytically, the associated linear system presented at (28) can be transformed to distributed delay form [11] by using the inverse of the stationary delay $\overline{\tau}_i(z) = \vartheta$ with the help of (6)

$$\mathbf{x}''(t) + \mathbf{D}\mathbf{x}'(t) + (\mathbf{K} + \delta\mathbf{C})\mathbf{x}(t) = \delta \sum_{i=1}^{Z} \int_{\overline{\tau}_{i,\min}}^{\overline{\tau}_{i,\max}} \mathbf{C}_i(z_i(\vartheta))\mathbf{x}(t-\vartheta)|z_i'(\vartheta)|\mathrm{d}\vartheta, \tag{40}$$

where in this simple case $\overline{\tau}_{i,\min} = \min(\varphi_{p,i}(z_0)/\nu, \varphi_{p,i}(1/2)/\nu)$ and $\overline{\tau}_{i,\max} = \max(\varphi_{p,i}(z_0)/\nu, \varphi_{p,i}(1/2)/\nu)$. The inverse is

$$z_i(\vartheta) = \frac{z_0}{(1-z_0)\mathrm{e}^{\gamma_i(\vartheta)} + z_0}, \quad \gamma_i(\vartheta) = 2\frac{\vartheta\nu + \varphi_{p,i,0}}{\tan\eta_i - \tan\eta_{i+1}}. \tag{41}$$

Equation (40) induces the following characteristic equation

$$\det(\mathbf{I}\lambda^2 + \mathbf{D}\lambda + (\mathbf{K} + \delta\mathbf{C}) - \delta \sum_{i=1}^{Z} \int_{-\infty}^{\infty} w_i(\vartheta)\mathbf{C}_i(z_i(\vartheta))\mathrm{e}^{-\lambda\vartheta}|z_i'(\vartheta)|\mathrm{d}\vartheta) \equiv 0, \tag{42}$$

where the window function is $w_i(\vartheta) = H(\vartheta - \overline{\tau}_{i,\min}) - H(\vartheta - \overline{\tau}_{i,\max})$ and $H(\vartheta)$ represents the Heaviside step function. With the substitution of $\lambda = \sigma + \mathrm{i}\omega$ all possible points can be investigated keeping in mind at the stability border $\lambda = \mathrm{i}\omega$. Thus, the sum and the integral become similar to Fourier transformation lifting out the decaying part of the characteristic exponent. Thus, the characteristic equation (42) has the form as

$$\det(\mathbf{I}(\sigma+\mathrm{i}\omega)^2 + \mathbf{D}(\sigma+\mathrm{i}\omega) + (\mathbf{K}+\delta\mathbf{C}) - \delta\mathbf{w}(\sigma,\omega)\star\mathbf{c}_1(\omega)) \equiv 0, \tag{43}$$

where $\mathbf{w}(\sigma,\omega) = \mathrm{row}_i(\mathscr{F}\{\mathrm{e}^{-\sigma\vartheta}w_i(\vartheta)\mathbf{I}\}(\omega))$, $\mathbf{c}_1(\omega) = \mathrm{col}_i(\mathscr{F}\{\mathbf{C}_i(z_i(\vartheta))|z_i'(\vartheta)|\}(\omega))$ and $\star$ denotes convolution in frequency domain. This form might give opportunity to find tilted lines along the lenses gathers showed in Fig. 3.

CONCLUSIONS

This work was motivated by the undiscovered regenerative dynamics of drill bits in deep drilling processes. We showed that, considering a 2 DoF model, it is possible to optimize the geometry of the drill bit in order to have either a robustly stable or a robustly unstable drilling process by only changing the variation of the helix angle for the cutting edges. Stable drilling can keep the tool life long, while unstable drilling process might help to cut hard earth crust material more effectively with percussive drilling. After the analytical derivation of the dimensionless governing equation that leads to a distributed delay system, a sample semi-analytical calculation presented the exploration of the intricate behaviour of the drilling process.

ACKNOWLEDGMENT

This research was partially supported by the Hungarian National Science Foundation under grant OTKA K83890, K101714 and by the EU FP7 Dynxperts (260073/FP7-2010-NMP-ICT-FoF).

REFERENCES

[1] Tucker, W., and Wang, C., 1999. "An integrated model for drill-string dynamics". *Journal of Sound and Vibration,* ***224(1)***, pp. 123–165.

[2] Richarda, T., Germay, C., and Detournay, E., 2004. "Self-excited stickslip oscillations of drill bits". *Comptes Rendus Mcanique,* ***332***, pp. 619–626.

[3] Karkoub, M., Abdel-Magid, Y., and Balachandran, B., 2009. "Drill-string torsional vibration suppression using ga optimized controllers". *Journal of Canadian Petroleum Technology,* ***48(12)***, pp. 32–38.

[4] Silveira, M., and Wiercigroch, M., 2009. "Low dimensional models for stick-slip vibration of drill-strings". *Journal of Physics: Conference Series,* ***181(1)***, p. 012056.

[5] Tlusty, J., and Spacek, L., 1954. *Self-excited vibrations on machine tools*. Nakl. CSAV, Prague. in Czech.

[6] Tobias, S., 1965. *Machine-tool Vibration*. Blackie, Glasgow.

[7] Hale, J., 1977. *Theory of functional differential equations*. Springer-Verlag, New York.

[8] Stépán, G., 1989. *Retarded dynamical systems*. Longman, London.

[9] Farkas, M., 1994. *Periodic Motions*. Springer-Verlag, Berlin and New York.

[10] Bellen, A., and Zennaro, M., 2003. *Numerical Methods for Delay Differential Equations*. Oxford University Press.

[11] Dombovari, Z., and Stepan, G., 2012. "The effect on helix angle variation on milling stability". *Journal of Manufacturing Science and Engineering,* ***134(5)***, pp. 051015(1)–051015(6).

[12] Voronov, S., Guskov, A., Kvashnin, A., Butcher, E., and Sinha, S., 2007. "Influence of torsional motion on the axial vibrations of a drilling tool". *Journal of computational and nonlinear dynamics,* ***2(1)***, pp. 55–64.

[13] Dombovari, Z., Altintas, Y., and Stepan, G., 2010. "The effect of serration on mechanics and stability of milling cutters". *International Journal of Machine Tools and Manufacture,* ***50***(6), pp. 511 – 520.

[14] Zatarain, M., Muñoa, J., Peigné, G., and Insperger, T., 2006. "Analysis of the influence of mill helix angle on chatter stability". *CIRP Annals - Manufacturing Technology,* ***55***, pp. 365–368.

[15] Bachrathy, D., and Stepan, G., 2011. "Bisection method in higher dimensions and the efficiency number". *Periodica Polytechnica, Mechanical Engineering,* ***56(2)***, pp. 81–86.

